

POLYANILINE INTERCALATED INTO ZEOLITES, ZIRCONIUM PHOSPHATE AND ZIRCONIUM ARSENATE

TE-CHUAN CHANG

Department of Applied Chemistry, Chung Cheng Institute of Technology, Taoyuan, Taiwan

AND

SHIH-YENG HO AND KUEI-JUNG CHAO

Department of Chemistry, National Tsinghua University, Hsinchu, Taiwan

Aniline (or aniline hydrochloride) was intercalated into zeolite, zirconium phosphate and zirconium arsenate (proton form and sodium form) and subsequently oxidized to polyaniline (PAN) by ammonium peroxodisulphate. The structure of PAN in the host was studied by electron paramagnetic resonance spectroscopy. PAN in the host gave a free-radical EPR signal at 2.0035–2.0037 for the hydrogen or 2.0047–2.0049 for the sodium form of the host, similarly to the emeraldine salt (PAN-2S) or emeraldine base (PAN-2A) form of PAN. Saturation occurs in PAN-HZ and PAN-HS. In contrast, the intrachannel PAN in HY was unsaturated under the same conditions. Conduction in PAN-HZ and PAN-HS was predominately carried out by variable-range hopping and tunnelling respectively, and PAN-HY showed insulating properties.

INTRODUCTION

The encapsulation of conjugated polymers in a crystalline microporous inorganic host has recently received extensive attention. Several studies have been reported on polyaniline (PAN), polypyrrole, polyacrylonitrile and polythiophene in caged zeolite¹ and layered montmorillonite,² α -zirconium phosphate,³ fluorohectorite,⁴ FeOCl⁵ and V₂O₅⁵ for the purpose of controlling the molecular alignment of conducting polymer chains.

Zeolites consist of an open aluminosilicate framework with pore sizes in the range 0.3–0.8 nm and possess a capacity for cation exchange depending on their aluminium content. Crystalline α -zirconium phosphate (HZ) and α -zirconium arsenate (HS) with layered structures, a high preference for Brønsted bases and a high ion-exchange capacity (6.64 meq. g⁻¹ for HZ⁶ and 5.14 meq. g⁻¹ for HS⁷) can be employed as the host lattice for aniline. Therefore, zeolite, HZ and HS offer convenient vehicles for the polymerization of aniline in their intrachannel or interlayer spaces.

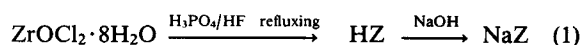
A granular polymeric metal model,⁸ with the conductivity states of metallic particles embedded in an unprotonated insulating sea, has been proposed. In addition, evidence for disorder has been pointed out, and it has been suggested that a Fermi glass might be more

appropriate.⁹ Recently it was confined by a spin dynamics technique with magnetic resonance that conductivity (σ) was dominated by the interchain diffusion rate.¹⁰ Therefore, spin dynamics enable us to study the conductivity on a microscopic scale. In this paper we report the spin dynamics and conductivity of PAN included inside the host system.

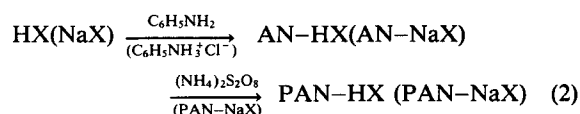
EXPERIMENTAL

A binder-free zeolite NaY (Si/Al = 2.41) was obtained from Strem Chemical. The ammonium form of the zeolite (NH₄Y) was obtained by ion exchanging NaY (2 g) with NH₄Cl (0.1 M, 4 × 200 ml) for 5 h. The zeolite NH₄Y was heated in a stream of oxygen (1 K min⁻¹, 8 h at 370 K; 4 h at 670 K) and evacuated for 2 h at 10⁻⁵ Torr (1 Torr = 133.3 Pa) followed by cooling, resulting in HY (H₄₆Na₁₀Y, subscripts indicate cations per unit cell). The hydrogen form of crystalline α -zirconium phosphate (HZ) and α -zirconium arsenate (HS) were prepared by decomposition of zirconium fluoro complexes of phosphoric acid and arsenic acid. Sodium form zirconium phosphate (NaZ) and zirconium arsonate (NaS) were obtained by titrating HZ and HS with the 0.1 M NaCl–0.1 M NaOH

solution,^{12,13} according to the equation



The aniline molecule was encapsulated into the intrachannel of HY as described.⁵ The aniline molecule was encapsulated into the interlayer space of HZ (or HS) by using the following procedure. Amounts of 2g each of HZ and HS were suspended in water, aniline was slowly added with stirring, the suspension was left to stand overnight and the AN-HZ and AN-HS were obtained. NaY, NaZ or NaS was exchanged with aniline hydrochloride at 25 °C with shaking for 6 h. Excess salt was removed by washing. The loaded aniline was subsequently oxidized with ammonium peroxodisulphate to PAN-host, stirring at 0 °C under nitrogen for 24 h. The green solids were isolated by centrifugation, washed with deionized water and dried. The reaction scheme is as follows:



ESR spectra were obtained on a Bruker ER 200D 10/12 EPR spectrometer. The powdered samples were introduced into an EPR tube that was connected to a vacuum system. The spin concentration of PAN-hosts was determined by double integration of the first-derivative signal, using 2,2-diphenyl-1-picrylhydrazyl (DPPH) as a standard. The spin-lattice and spin-spin relaxation times, T_1 and T_2 , respectively, were determined by saturation methods.¹⁴ The electrical conductivities were determined by a four-probe method on compressed pellets at temperatures between 130 and 273 K.

RESULTS AND DISCUSSION

g Factor

A free-radical peak appeared in the EPR spectra of the PAN-hosts. No free-radical signal was found in the

EPR spectra of either the hosts or aniline-loaded host samples. The *g* value of the EPR signal is a function of the molecular motion, the paramagnetic properties and the symmetry of ions.¹⁵ The *g* factor of an electron near a carbon-hydrogen bond is about 2.0031, whereas it is 2.0054 for an electron near a nitrogen-hydrogen bond.¹⁶ The *g* factors of PAN-HY, PAN-HZ and PAN-HS lie in the range 2.0035–2.0033 (Table 1), indicating that the spins are delocalized over at least one ring and nitrogen repeating unit (*ca* 5 Å), since the value of *g* (2.0035–2.0037) corresponds closely to the arithmetic mean of the *g* factors of the six carbons and one nitrogen in the repeat unit. In contrast, *g* factors of PAN intercalated in a sodium-form host (2.0047–2.0049) are close to 2.0054, implying that the radicals are localized to nitrogen sites only.¹⁷

Peak-to-peak linewidth (ΔH_{pp})

The smaller EPR peak-to-peak linewidth for PAN-HZ ($\Delta H_{pp} = 0.72$ G vs 2.62 G for PAN-NaZ at 293 K) suggests more motional narrowing and, hence, increased delocalization. PAN in proton-form hosts were shown to be mainly in the salt form according to the *g* factors. The values of ΔH for PAN-HY (8.84 G), PAN-HZ (0.72 G) and PAN-HS (1.38 G) are larger than that for PAN-2S (0.4 G),¹⁸ probably owing to different protonation levels¹⁹ and intercalation effects of the hosts.²⁰ In comparison with the EPR resonance of PAN-2A ($\Delta H_{pp} = 8.5$ G),¹⁸ the broad ΔH_{pp} of PAN-NaY (12.37 G) corresponds to the intercalated base form of PAN.

The EPR peak-to-peak linewidth of PAN in proton-form hosts decreases monotonically as the temperature increases from 110 to 293 K (Figure 1). This indicates that the linewidth is determined by motional narrowing; however, that of PAN-2S shows very little temperature dependence.¹⁹

Spin concentration (N_s)

The EPR peak intensity was calculated as the product $\Delta H_{pp}^2 h$, where ΔH_{pp} is the peak-to-peak linewidth and

Table 1. EPR data and electrical conductivities, σ , of different samples at 298 K^a

Sample	<i>g</i>	ΔH_{pp} (G)	N_s (10^{18} spins g ⁻¹)	T_1 (10^{-8} s)	T_2 (10^{-8} s)	σ (S cm ⁻¹)	E_a (eV)
PAN-NaY	2.0047	12.37	6.93	—	—	$< 10^{-7}$	—
PAN-NaZ	2.0049	2.62	11.97	—	—	3×10^{-6}	—
PAN-NaS	2.0049	2.62	10.32	—	—	7×10^{-6}	—
PAN-HY	2.0035	8.84	13.80	< 43	0.6	$< 10^{-7}$	—
PAN-HZ	2.0033	0.72	51.34	43	2.3	2×10^{-3}	0.085
PAN-HS	2.0033	1.38	23.90	167	1.5	9×10^{-4}	0.071

^a ΔH_{pp} = peak-to-peak linewidth, N_s = spin concentration, T_1 = spin-lattice relaxation time, T_2 = spin-spin relaxation time and E_a = activation energy.

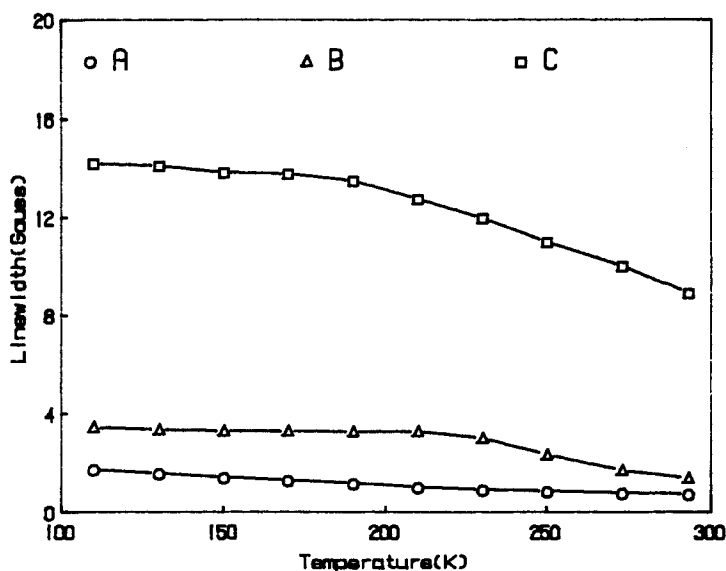


Figure 1. Temperature dependence of the linewidth ΔH_{pp} (G) of samples (A) PAN-HZ, (B) PAN-HS and (C) PAN-HY

h is peak-to-peak height. The spin concentrations (N_S) of intercalated PAN in HY, HZ and HS, calculated from the signal intensity at 297 K by comparison with DPPH under the same conditions, are 13.8×10^{18} , 51.3×10^{18} and 23.9×10^{18} spins g^{-1} respectively, but smaller than that in bulk PAN-2S (10^{21} – 10^{22}

spins g^{-1}).²⁰ The spin concentrations of intercalated PAN in sodium-form hosts are smaller than those in proton-form hosts (Table 1).

Figure 2 shows the temperature dependence of the relative signal intensity $I_r = I(TK)/I(293 K)$, which is proportional to the magnetic susceptibility.²¹ I_r grad-

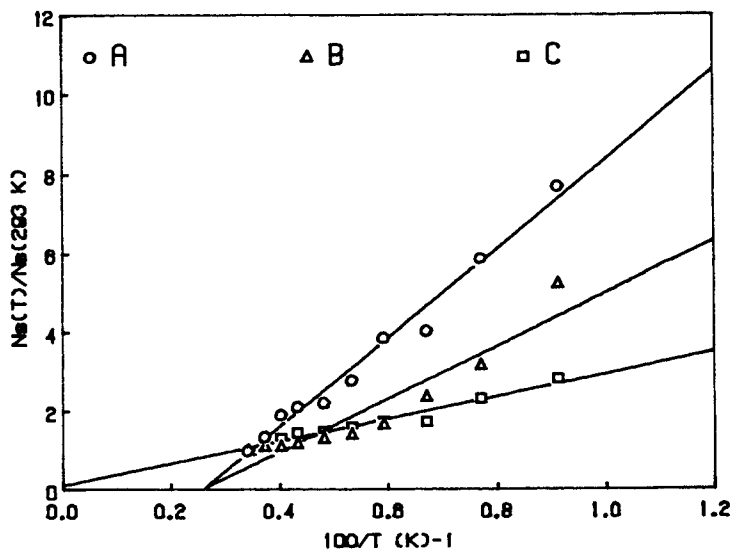


Figure 2. Temperature dependence of the relative signal intensity $I(TK)/I(293 K)$ of samples (A) PAN-HZ, (B) PAN-HS and (C) PAN-HY

ually increased with decrease in temperature, similarly to the emeraldine salt.¹⁹ The I_r value PAN-HY shows Curie behaviour ($I_r = C/T$) throughout the temperature range investigated (110–293 K), whereas the I_r values of PAN-HZ and PAN-HS show Curie-Weiss behaviour [$I_r = C/(T - \Theta)$], where Θ corrects the temperature for the non-zero intercept. The value of the intercept is due to intermolecular interactions.²¹ In these systems, it is indicated that virtually no defects are present in PAN-HY and a small concentration of paramagnetic defects are present in PAN-HZ and PAN-HS.

Spin-lattice relaxation time (T_1) and spin-spin relaxation time (T_2)

In order to determine the spin-lattice and spin-spin relaxation times (T_1 and T_2 , respectively), a series of EPR spectra were recorded with the power varying from a condition of negligible saturation to one of pronounced saturation.¹⁴ The spin-spin relaxation time T_2 is calculated from the linewidth below saturation (i.e. ΔH_{pp}^0) by means of the expression

$$T_2 = \frac{1.3131 \times 10^{-7}}{g \Delta H_{pp}^0} \quad (3)$$

and the spin-lattice relaxation time T_1 is calculated from the equation

$$T_1 = \frac{0.9848 \times 10^{-7} \Delta H_{pp}^0 [1/(s-1)H_1^2]}{g} \quad (4)$$

where H_1 is the microwave amplitude and S is the

saturation factor. The best result is obtained when equation (4) is used for power levels that are only moderately above saturation. The plot of the square root of the microwave power P against the peak-to-peak amplitude of the derivative spectrum Y_m is shown in Figure 3.

Heterogeneous saturation occurs in PAN-HZ and PAN-HS as shown in Figure 3(A) and (B). The EPR line arises from the overlapping of several individual lines. The spin-lattice and spin-spin relaxation times are given in Table 1. According to Mizoguchi and co-workers^{9,22} one has $T_1 = T_2$ at high dopant levels (y) and $T_2 \gg T_1$ for $y < 0.3$, so that the interlayered PAN has a higher dopant level in HZ than in HS. Surprisingly, the intrachannel PAN in HY is unsaturated under the same conditions, although PAN-HY has a broader linewidth of the EPR resonance than PAN-HZ and PAN-HS. The most likely explanation is an intrinsic dipolar interaction between the PAN chains and the charged zeolite channel walls,¹ that is broadened by fast relaxation.

Conductivity (σ)

In previous studies, equations related to specific composites and various models for electrical conduction in composites have been suggested. However, the precise conducting mechanisms in polymer systems are not fully understood, since they are influenced by factors such as the dopant level, the morphology of the polymers, orientation of conducting species and temperature. The conductivities at 25 °C for various conducting

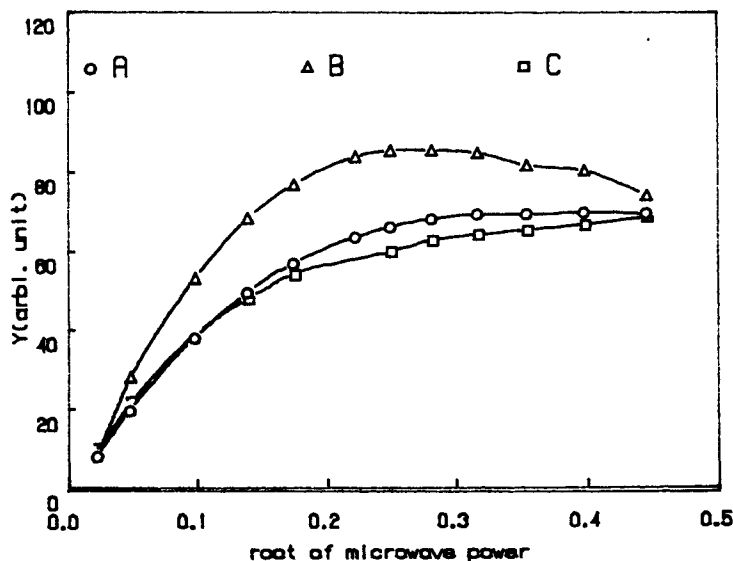


Figure 3. Saturation curves obtained by plotting peak-to-peak amplitude Y_m against the square root of microwave power P ($W^{1/2}$). (A) PAN-HZ; (B) PAN-HS; (C) PAN-HY

polymers are given in Table 1. The electrical conductivity as a function of temperature based on the hopping conduction mechanism has been given by Mott²³ and Greaves.²⁴ However, Mott's equation is based on the assumption that the concentration of charge carriers has nothing to do with the temperature. According to Greaves, variable-range hopping (VRH) conduction is represented by

$$\sigma = \sigma_0(T) \exp(-B/T^{1/4}) \quad (5)$$

where B is a constant. On the other hand, the electrical conductivity as a function of temperature is given by Matares' equation:²⁵

$$\sigma = AT^{1/2} \exp(E_a/kT) \quad (6)$$

where A is constant and E is the height of the potential barrier. This equation was derived for a system including grain boundary barriers. Also, Zeller²⁶ and Orton and Powell²⁷ have shown that tunnelling and thermionic emission conduction can be expressed by the

following two equations, respectively;

$$\sigma \approx \exp(-A/T^{1/2}) \quad (7)$$

$$\sigma = \sigma_0 T^{-1/2} \exp(-E_a/kT) \quad (8)$$

Measurements of electrical conductivity were performed by a four-probe technique at temperatures from 130 to 273 K. The temperature dependence of the conductivity of the pressed-pellet samples is shown in Figure 4. As can be seen, the conductivity increases linearly with increase in temperature, satisfying the Arrhenius equation, $\sigma = \sigma_0 \exp(-E_a/kT)$. E_a values for PAN-HZ and PAN-HS were obtained from the slope of the straight line in Figure 4 and were 0.085 and 0.070 eV, respectively. The temperature dependencies of the electrical conductivity of PAN-HZ and PAN-HS, according to equations (5)–(8) show that the conduction of PAN-HZ and PAN-HS is predominately carried out by variable range hopping and tunnelling respectively. At concentrations of metallic domains in PAN-HZ above the percolation threshold,

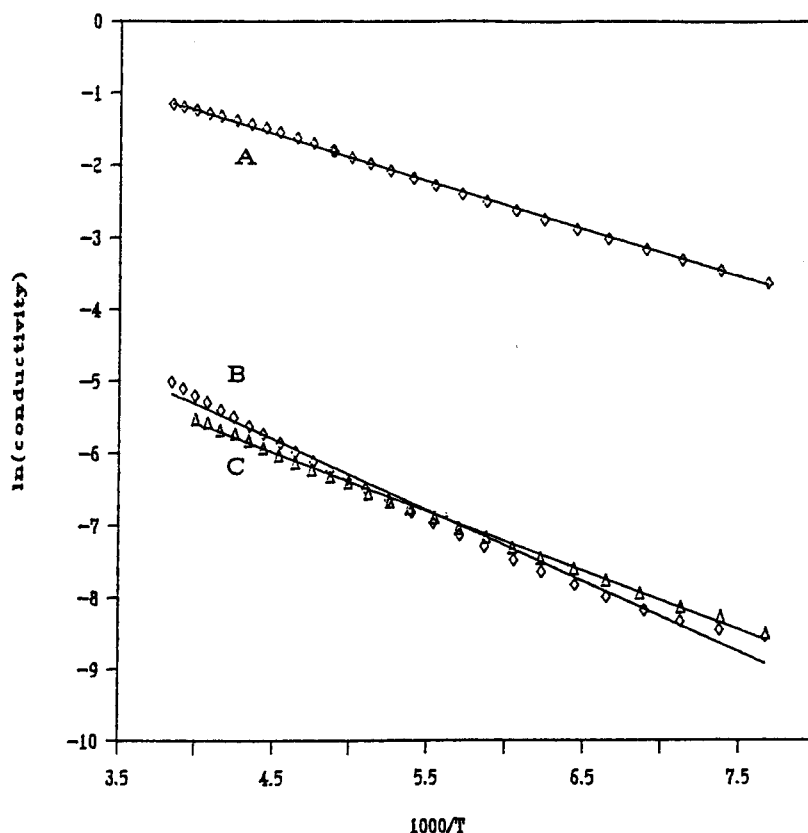


Figure 4. Temperature dependence of electrical conductivities σ of samples (A) PAN-HZ (B) PAN-HS and (C) PAN-HY. The straight lines show the semiconducting relations $\sigma = \sigma_0 \exp(-E_a/kT)$

the conductivity has a temperature dependence like that of VRH in three dimensions.^{28,29} In contrast, at concentrations of metallic domains in PAN-HS below the percolation threshold, the conductivity is dominated by tunnelling conduction.²⁹ The dimensions of the HY zeolite intrachannels are such that only one polymeric chain can fit. Therefore, the polymer chains cannot interact with one another in the zeolite host, resulting in good insulating properties.³⁰

CONCLUSION

The *g* values of polyaniline in the hydrogen or sodium form of the host gave a free-radical EPR signal which is similar to that for the emeraldine salt or emeraldine base, respectively. The spins in isolated single oligomeric conjugated PAN in HY do not saturate easily, which is due to an intrinsic bipolar interaction, although almost no defects were present in PAN-HY. Therefore, PAN-HY shows good insulating properties. The encapsulated PAN in α -zirconium phosphate has higher dopant level than in α -zirconium arsenate from the peak-to-peak linewidth, spin dynamics and conductivity. The encapsulated PAN in the galleries of layered hosts results in highly oriented films; high anisotropic structures are obtained.

ACKNOWLEDGEMENT

We thank the National Science Council of the Republic of China for support of this research.

REFERENCES

1. T. Bein and P. Enzel, *Mol. Cryst. Liq. Cryst.* **181**, 315 (1990); T. Bein and P. Enzel, *Synth. Met.* **29**, E163 (1989); T. Bein and P. Enzel, *J. Phys. Chem.* **93**, 6270 (1989); T. Bein and P. Enzel, *J. Chem. Soc., Chem. Commun.* 1326 (1989); T. Bein and P. Enzel, *Angew. Chem., Int. Ed. Engl.* **28**, 1692 (1989).
2. T. C. Chang, S. Y. Ho and K. J. Chao, *J. Chin. Chem. Soc.* **39**, 209 (1992); H. Inoue and H. Yoneyama, *J. Electroanal. Chem.* **233**, 291 (1987).
3. K. J. Chao, T. C. Chang and S. Y. Ho, *J. Mater. Chem.* **3**, 427 (1993).
4. V. Mehrotra and E. M. Giannelis, *Solid State Commun.* **77**, 155 (1991).
5. M. G. Kanatzidis, L. M. Tonge, T. J. Marks, H. O. Marcy and C. R. Kannewurf, *J. Am. Chem. Soc.* **109**, 3797 (1987); M. G. Kanatzidis, C. G. Wu, H. O. Marcy and C. R. Kannewurf, *J. Am. Chem. Soc.* **111**, 4139 (1989).
6. J. M. Troup and A. Clearfield, *Inorg. Chem.* **16**, 331 (1977).
7. A. Clearfield, G. D. Smith and B. Hammond, *J. Inorg. Nucl. Chem.* **30**, 277 (1968).
8. J. M. Ginder, A. F. Richter, A. G. MacDiarmid and A. J. Epstein, *Solid State Commun.* **63**, 97 (1987).
9. M. Nechtschein, F. Genoud, C. Menardo, K. Mizoguchi, J. P. Travers and B. Villet, *Synth. Met.* **29**, E211 (1989).
10. K. Mizoguchi, M. Nechtschein and J. P. Travers, *Synth. Met.* **41-43**, 113 (1991).
11. A. Alberti, U. Costantino, S. Allulli and M. A. Massucci, *J. Inorg. Nucl. Chem.* **37**, 1779 (1975).
12. U. Costantino, *J. Chem. Soc., Dalton Trans.* 402 (1979).
13. A. Clearfield and J. A. Stynes, *J. Inorg. Nucl. Chem.* **26**, 117 (1964); A. Clearfield and A. S. Medina, *J. Inorg. Nucl. Chem.* **32**, 2775 (1970).
14. C. P. Poole, *Electron Spin Resonance*, 2nd ed. Wiley, New York (1982).
15. J. W. Stucki and W. L. Banwart, *Advanced Chemical Methods for Soil and Clay Mineral Research*. Reidel, Dordrecht (1980).
16. J. R. Morton, *Chem. Rev.* **64**, 453 (1964).
17. Z. H. Wang, H. H. S. Javadi, A. Ray, A. G. MacDiarmid and A. J. Epstein, *Phys. Rev. B* **42**, 5411 (1990); Z. H. Wang, A. Ray, A. G. MacDiarmid and A. J. Epstein, *Phys. Rev. B* **43**, 4373 (1991).
18. M. Inoue, R. E. Navarro and M. B. Inoue, *Polym. Bull.* **27**, 435 (1992).
19. E. H. S. Javadi, R. Laversannc, A. J. Epstein, R. K. Kohli, E. M. Scheerr and A. G. MacDiarmid, *Synth. Met.* **29**, E439 (1989).
20. T. A. Skotheim, *Handbook of Conducting Polymers*. Marcel Dekker, New York. (1986); J. C. W. Chien, *Polyacetylene Chemistry, Physics and Material Science*, p. 187. Academic Press, New York (1984).
21. M. Iido, T. Asaji, M. Inoue and H. Grijalva, *Bull. Chem. Soc. Jpn.* **64**, 1509 (1991); R. S. Drago, *Physical Methods in Chemistry*, p. 416. W. B. Saunders, Philadelphia, PA (1977).
22. K. Mizoguchi, M. Nechtschein, J. P. Travers and C. Menardo, *Synth. Met.* **29**, E417 (1989).
23. N. F. Mott, *J. Non-Cryst. Solids* **1**, 1 (1968).
24. G. N. Greaves, *J. Non-Cryst. Solids* **11**, 427 (1973).
25. M. F. Matare, *J. Appl. Phys.* **56**, 2605 (1984).
26. H. R. Zeller, *Phys. Rev. Lett.* **28**, 1452 (1972).
27. J. W. Orton and M. J. Powell, *Rep. Prog. Phys.* **43**, 1263 (1980).
28. F. Zuo, M. Angelopoulos, A. G. MacDiarmid and A. J. Epstein, *Phys. Rev. B* **39**, 3570 (1989).
29. L. Yu, *Solitons and Polarons in Conducting Polymers*, p. 124. World Scientific, Singapore (1988).
30. M. G. Kanatzidis, *Chem. Eng. News* **68**, 36 (1990).